A Liquid Crystal-Based Fourier Optical Spectrum Analyzer

Yan-Qing Lu, *Member, IEEE,*, Charles Wong, and Shin-Tson Wu, *Fellow, IEEE*

***Abstract*—We propose a liquid crystal (LC)-based cost-effective Fourier optical spectrum analyzer (FOSA) without moving parts. Unlike normal spectrometers, the LC FOSA retrieves the spectrum's Fourier coefficients instead of the direct spectrum measurement by changing different LC states in a number of stages. Besides the common applications, the LC FOSA can precisely read and recover the envelope of a dense wavelength-division-multiplexing spectrum to act as a spectral monitor and then work with a gain-flattening device to control the optical network instantly and dynamically.**

***Index Terms*—Dense wavelength-division multiplexing (DWDM), dynamic gain-flattening filter (DGFF), Fourier transform spectrometer, liquid crystal (LC) devices, optical spectrum analyzer (OSA).**

THE DYNAMIC gain-flattening filter (DGFF) plays an important role in the dense wavelength-division multiplexing (DWDM) fiber-optic communication networks. With the help of DGFF, architectures that were once static and inflexible become dynamic and agile so that they could correct the imbalances in the power of signal channels. These imbalances may originate from many sources but the most common reason is the nonuniform gain spectrum of the erbium-doped fiber amplifier (EDFA). In long-haul networks, where many amplifiers are cascaded, the accumulated channel power discrepancies may severely restrict the available bandwidth or even render normal communication impossible [1]–[6].

Several technologies have been proposed to dynamically adapt the power distribution across DWDM channels. For example, the fiber Bragg grating [2], acoustooptic filter [3], fiber loop-mirror [4], and Fourier sinusoidal filters based on Mach–Zehnder interference [5] or liquid crystal (LC) polarization interferences [6]. However, for realizing the dynamic control, an optical spectrum analyzer (OSA) is prerequisite to monitor the spectral profile and then feed it back to the DGFF for signal processing. The common telecommunication-grade OSA is a diffraction-grating-based spectrometer that has extremely high resolution and broad spectral range, but is usually bulky and expensive. It is very beneficial and quite urgent to develop the compact and cost-effective OSAs for DGFF and other applications. In fact, because of the attractive low cost and versatile properties of LCs, the potable LC-based Fourier transform spectrometer has recently been demonstrated [7]. However, due to the continuous phase retardation change in the LC wedge, it is difficult to realize the digital control, it also requires complicated image treatment, which may increase the system cost. As a result, it is not very suitable for the telecommunication applications.

Manuscript received June 13, 2003; revised November 26, 2003. This work was supported by the Air Force Office of Scientific Research (AFOSR) under Contract F49620-01-1-0377.

Y.-Q. Lu and S.-T. Wu are with the School of Optics/CREOL, University of Central Florida, Orlando, FL 32816 USA (e-mail: LYQ@ieee.org).

C. Wong is with Chorum Technologies, Inc., Richardson, TX 75081 USA.

Digital Object Identifier 10.1109/LPT.2004.823723

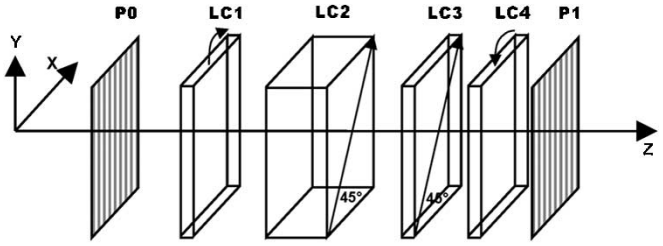

Fig. 1. Schematic diagram of a single-stage LC FOSA.

In this letter, we proposed a static LC-based Fourier optical spectrum analyzer (FOSA) with adjustable resolution and the capability of digital controlling. Besides the common spectrometer applications, this LC FOSA can work with the DGFF to monitor and protect a DWDM system. Furthermore, it is even possible to integrate the filter function into this LC FOSA to build a self-adaptive DGFF/OSA.

Fig. 1 shows the schematic diagram of a single-stage LC FOSA which contains four LC cells sandwiched between a pair of parallel polarizer P0 and analyzer P1. LC1 and LC4 are two twisted nematic (TN) LC cells with 45° twist angle. In LC1, the polarization of the incident light, which is polarized by P0, follows the twist of LC molecules so that it is rotated by 45°. The LC4 is similar to LC1 but with the opposite twist direction so that it rotates the light polarization by -45°, as shown in Fig. 1. When a sufficient AC voltage is applied to LC1 and LC4, the polarization guiding effect is disrupted and, thus, they just act like optical glasses. Besides TN cells, LC1 and LC4 could be other types of polarization controllers. For example, it can be a Faraday rotator or an electrooptic crystal rotator [8]. However, the TN LC has the advantages of simplicity, inexpensiveness, and wavelength-independence. LC2 is a high-birefringence LC with fixed phase retardation between the ordinary beam and the extraordinary beam. Its optical axis is 45° with respect to the X and Y axes. Obviously, LC2 could also be a birefringent crystal. However, the birefringence of a normal crystal such as quartz $(\Delta n = 0.01)$ is much lower than that of an LC [9], thus, the LC is preferred in some applications to avoid a bulky package. LC3 is another LC cell with the electrically controlled birefringence that can induce either full-wave or quarter-wave phase retardation between two polarization states. Its optical axis is parallel to that of LC2.

1041-1135/04$20.00 © 2004 IEEE

With the combination of these elements, three system states could be generated.

State 1: LC1 and LC4 are both in the voltage-OFF state. The polarization of the incident light is rotated along the LC2 and LC3's optical axes and then rotated back along P1 by LC4. In this case, all lights in the studied frequency range Δf can fully pass. The detected light intensity is

$$I1 = \int_{\Delta f} s(f)df \tag{1}$$

where $s(f)$ is the incident light spectrum.

State 2: LC1 and LC4 are both in the voltage-ON state so that they do not affect the light polarizations. LC3 now acts as a full-wave plate. In this case, the incoming light is linearly polarized along the Y axis by P0. It is decomposed into two equal orthogonal polarized components in LC2. P1 recombines the two polarization components and results in an optical interference between them. The transmittance of this interference filter is [10]

$$\begin{aligned} T(f) &= \cos^2\left(\frac{\Gamma}{2}\right) = \frac{1}{2}(1+\cos\Gamma) \\ &= \frac{1}{2}\left[1+\cos\left(\frac{2\pi f}{\mathrm{FSR}}\right)\right] \end{aligned} \tag{2}$$

where $\Gamma = 2\pi f/\mathrm{FSR}$ is the phase retardation of LC2 between two different polarizations and FSR is the free spectral range of this filter.

In this circumstance, the detectable light intensity is

$$I2 = \frac{1}{2}\int_{\Delta f} s(f)df + \frac{1}{2}\int_{\Delta f} s(f)\cos\left(\frac{2\pi f}{\mathrm{FSR}}\right)df. \tag{3}$$

State 3: The LC3 now works as a quarter-wave plate but others are in the same status as those in State 2. The phase retardation is, thus, increased by $\pi/2$ so that the detected light intensity becomes

$$I3 = \frac{1}{2}\int_{\Delta f} s(f)df + \frac{1}{2}\int_{\Delta f} s(f)\sin\left(\frac{2\pi f}{\mathrm{FSR}}\right)df. \tag{4}$$

On the other hand, an arbitrary input spectrum $s(f)$ in a specific frequency range Δf can be expressed as a Fourier series if virtually expanding $s(f)$ with a frequency period (FP)

$$\begin{aligned} s(f) = a_0 + \sum_{m=1}^{N}\Bigg[a(m)\cos\left(\frac{2m\pi f}{\mathrm{FP}}\right) \\ + b(m)\sin\left(\frac{2m\pi f}{\mathrm{FP}}\right)\Bigg] \end{aligned} \tag{5}$$

$$\begin{cases} a_0 = \frac{1}{\mathrm{FP}}\int_{\Delta f} s(f)df \\ a(m) = \frac{2}{\mathrm{FP}}\int_{\Delta f} s(f)\cos\left(\frac{2m\pi f}{\mathrm{FP}}\right)df \\ b(m) = \frac{2}{\mathrm{FP}}\int_{\Delta f} s(f)\sin\left(\frac{2m\pi f}{\mathrm{FP}}\right)df. \end{cases} \tag{6}$$

Obviously, $s(f)$ can be reproduced from its Fourier coefficients. In fact, because of the typical asymmetrical twin peak structure of an EDFA gain profile, only about five Fourier items is enough for its spectrum recovery [5].

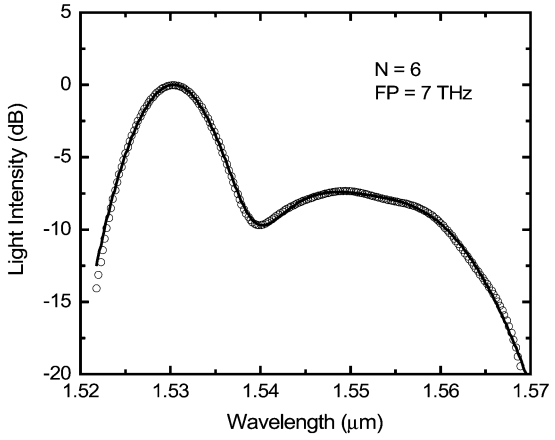

Fig. 2. Typical EDFA gain profile (solid line) and the reproduced spectrum curve (open circles) from the retrieved Fourier coefficients that are measured by a six-stage LC FOSA.

Comparing the above equations, $a(m), b(m)$, and a_0 in (6) are the same as those items in (1), (3), and (4) if the filter's $\mathrm{FSR} = \mathrm{FP}/m$. It means that the mth Fourier coefficients of the incident spectrum could be derived from I1, I2, and I3 by selecting a suitable FSR. As a consequence, the spectrum can be reproduced from its Fourier coefficients by employing sufficient stages of these sinusoidal interference filters, as described in Fig. 1. The whole LC FOSA is comprised of a number of stages that are packaged in serial or parallel. To increase the resolution which is determined by the stage number N, these stages can be aligned in a two-dimensional matrix. Owing to the similarity between different stages, it is very easy to control the LC FOSA digitally.

For evaluating the FOSA performance, the spectrum recovery of a typical EDFA gain spectrum, shown as the solid line in Fig. 2, is studied. The FP is 7 THz and only six stages are used. The open circle curve is the reproduced spectrum. From this figure, the spectrum is recovered very well, especially in the useful high-gain region. However, in the low-gain region, where the spectrum severely changes, the reading error increases. The discrepancy in the low wavelength end reaches 1.6 dB. This is due to the limitation of the system resolution, but it can be improved easily by employing more stages. For example, if a seven-stage FOSA is employed, the maximum discrepancy could be decreased to below 1 dB. The required stages in a practical FOSA should be determined by the tradeoff between resolution and cost.

However, in a real DWDM system, the data signals are carried in different frequency channels. The real spectrum that the FOSA needs to handle is the dense pin-like spectrum instead of the normal continuous curve. The spectrum envelope shows the intensity distribution across different channels. It is necessary to investigate the behavior of the LC FOSA for this application to ensure its capability in DWDM networks.

The DWDM spectrum $s(f)$ can be represented by the product of two parts: the envelope function $E(f)$ and a period function $g(f)$ with the frequency δf, where δf is just the frequency spacing between adjacent channels, e.g., 100 or 50 GHz. The

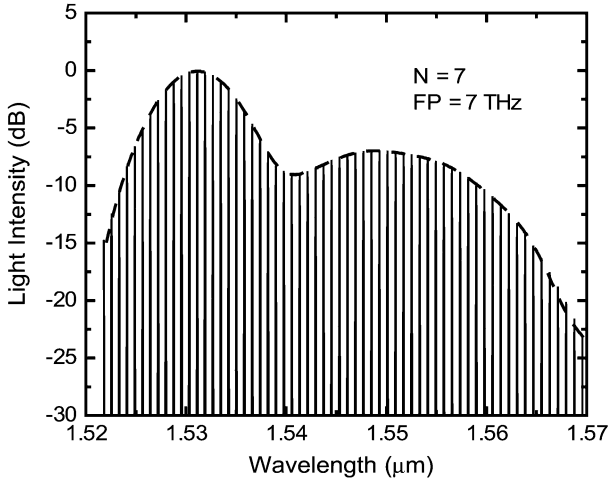

Fig. 3. DWDM spectrum and its envelope recovery by a seven-stage LC FOSA.

detected light intensity while $s(f)$ passing through an interference filter is

$$I = \frac{1}{2}\int_{\Delta f} E(f)g(f)df + \frac{1}{2}\int_{\Delta f} E(f)g(f)\cos\Gamma df. \quad (7)$$

As a periodic function, $g(f)$ could be expanded as $g(f) = g_0 + \sum_{m=1}^{\infty} g_m \cos(2m\pi f/\delta f)$, so

$$I = \frac{g_0}{2}\left[\int_{\Delta f} E(f)df + \int_{\Delta f} E(f)\cos\Gamma df\right] + \frac{1}{2}\sum_{m=1}^{\infty} g_m \left[\int_{\Delta f} E(f)\cos\left(\frac{2m\pi f}{\delta f}\right)df + \int_{\Delta f} E(f)\cos\left(\frac{2m\pi f}{\delta f}\right)\cos\left(\frac{2\pi f}{\mathrm{FSR}}\right)df\right]. \quad (8)$$

In a DWDM system, $\delta f \ll \mathrm{FSR}$, the slowly varying envelope approximation could be used so that the second part of (8) is neglectable. The detected DWDM spectrum intensity is just proportional to that of a continuous spectrum with the same envelope. In other words, what the FOSA can get is the DWDM spectrum's envelope with a fixed value offset in decibel scale, which is easy to be calibrated in a real device.

Fig. 3 shows the recovery of a DWDM spectrum with 100-GHz channel spacing. The FP is 7 THz and a seven-stage LC FOSA is used. The dashed curve is the obtained spectrum envelope, which coincides very well with the real spectrum. To further study the LC FOSA, some other DWDM spectra with different shapes and different channel spacing are also simulated. The results are very good indicating that the LC FOSA is an effective way to record the DWDM spectrum envelope. However, a real system does not always carry all DWDM channels. For example, a system may have four channels closely spaced at 1550 nm, and a single channel at 1530 nm. The LC FOSA is not able to resolve the closely spaced channels. It would, therefore, see four times the optical power at 1550 as 1530 nm, but this problem may be fixed by further treating the measured data with consideration of the channel occupation information.

Compared with the conventional OSAs, the LC FOSA has many advantages, e.g., it is static, economic, and digitally controllable. In addition, it still has a unique merit if working with a Fourier filter type DGFF [5], [6]. The DGFF, thus, can directly use the measured Fourier coefficients to tune the sinusoidal filters toward the target without a complicated algorithm to reproduce and analyze the spectrum. More attractively, because of the structural similarity between the LC-based DGFF [6] and LC FOSA, the functions of the gain-flattening filter and OSA could be combined together to make a novel self-adaptive filter/OSA. Such a multifunctional product should find many promising applications.

In summary, a low-cost static LC FOSA has been demonstrated. It can efficiently retrieve the Fourier coefficients of an input spectrum by changing the LC states in different stages. The spectral profile of the input light can, thus, be calculated with the Fourier series. In comparison with the current commercially available OSA, the LC FOSA has several advantages. In addition, the usage of LC FOSA is not limited to the fiber-optic field; other applications such as semiconductor characterization, chemical analysis, and biological detection are also promising.

REFERENCES

[1] B. J. Offrein, F. Horst, G. L. Bona, R. Germann, H. W. M. Salemink, and R. Beyeler, "Adaptive gain equalizer in high-index-contrast SiON technology," *IEEE Photon. Technol. Lett.*, vol. 12, pp. 504–506, May 2000.

[2] S. K. Liaw, K. P. Ho, and S. Chi, "Dynamic power-equalized EDFA module based on tunable fiber Bragg gratings," *IEEE Photon. Technol. Lett.*, vol. 11, pp. 797–799, July 1999.

[3] S. K. Yun, B. W. Lee, H. K. Kim, and B. Y. Kim, "Dynamic erbium-doped fiber amplifier based on active gain flattening with fiber acousto-optic tunable filters," *IEEE Photon. Technol. Lett.*, vol. 11, pp. 1229–1231, Oct. 1999.

[4] S. Li, K. S. Chiang, and W. A. Gambling, "Gain flattening of an erbium-doped fiber amplifier using a high-birefringence fiber loop mirror," *IEEE Photon. Technol. Lett.*, vol. 13, pp. 942–944, Sept. 2001.

[5] S. P. Parry, J. P. King, K. B. Roberts, N. E. Jolley, R. Keys, and J. Mun, "Dynamic gain equalization of EDFAs with Fourier filters," in *Proc. OSA Trends Optics and Photonics on Optical Amplifiers and Their Applications*, 1999, pp. 161–164.

[6] M. Xu, T. Huang, C. Mao, J. Y. Liu, K. Y. Wu, and C. Wong, "Dynamic Gain Equalizer for Optical Amplifiers," U.S. Patent 6 429 962, Aug. 6, 2002.

[7] G. Boer, T. Scharf, and R. Dandliker, "Compact static Fourier transform spectrometer with a large field of view based on liquid-crystal technology," *Appl. Opt.*, vol. 41, pp. 1400–1407, Mar. 2002.

[8] Y. Q. Lu, Z. L. Wan, Q. Wang, Y. X. Xi, and N. B. Ming, "Electro-optic effect of periodically poled optical superlattice $LiNbO_3$ and its applications," *Appl. Phys. Lett.*, vol. 77, pp. 3719–3721, Dec. 2000.

[9] S. T. Wu and D. K. Yang, *Reflective Liquid Crystal Displays*. New York: Wiley, 2001, ch. 2.

[10] I. C. Khoo and S. T. Wu, *Optics and Nonlinear Optics of Liquid Crystals*, Singapore: World Scientific, 1993, pp. 108–109.